Combustion and Flame 183 (2017) 157–165

Contents lists available at ScienceDirect

Combustion and Flame

journal homepage: www.elsevier.com/locate/combustflame

Two-stage heat release in nitromethane/air flame and its impact on laminar flame speed measurement

Mahdi Faghih, Zheng Chen*

SKLTCS, Department of Mechanics and Engineering Science, College of Engineering, Peking University, Beijing 100871, China

ARTICLE INFO

Article history:
Received 23 February 2017
Revised 9 May 2017
Accepted 11 May 2017

Keywords:
Nitromethane/air
Two-stage heat release
Laminar flame speed
Propagating spherical flame

ABSTRACT

In premixed flames of most hydrocarbon fuels, there is only one stage heat release. However, two-stage heat release occurs in premixed nitromethane/air flames under certain conditions. In this study, numerical simulations were conducted for one-dimensional planar and spherical nitromethane/air flames at different initial temperatures (423∼800 K), pressures (0.5∼10 atm) and equivalence ratios (0.5∼1.3). Using the planar flame, we investigated the characteristics of the two-stage heat release and identified elementary reactions involved in these two stages. It was found that the occurrence of two-stage heat release strongly depends on the equivalence ratio and that single-stage heat release occurs for very fuel-lean mixture. To demonstrate the key reactions involved in the second stage heat release, we modified the original chemical mechanism and compared the results predicted by different mechanisms. The second stage heat release was found to be mainly caused by the reaction NO+H→N+OH. Using the propagating spherical flame, we assessed the impact of two-stage heat release on the determination of laminar flame speed. The positive burned gas speed induced by the second stage heat release was shown to affect the accuracy of laminar flame speed determined by traditional method neglecting burned gas speed and using the density ratio at equilibrium condition. Alternative methods were proposed and used to correct the experimental data reported in the literature.

1. Introduction

Nitromethane (CH_3NO_2) can be used as a fuel additive in internal combustion engines (ICEs) and as a monopropellant in rocket engines. Blending nitromethane into gasoline helps to increase the octane number and to prevent knocking in direct-injected boosted gasoline engines [1]. Recent experiments showed that nitromethane addition to gasoline reduces soot formation but increases the emission of HCN and NO_x [2]. Besides, since nitromethane is the simplest nitro paraffin fuel, it is popularly used to study the combustion properties of liquid propellants [3].

Unlike the combustion of traditional fuels, nitromethane combustion proceeds via two or three steps. Hall and Wolfhard [4] first observed two luminous reaction zones in a low-pressure nitromethane/oxygen flame. Boyer and Kuo [3] simulated one-dimensional (1D) nitromethane combustion with surface vaporization. They identified three distinct reaction regions based upon the appearance and consumption of certain species. Nauclér et al. [5] found that fuel-rich nitromethane/air flames have two separate reaction zones according to their numerical simulation considering detailed chemistry. In shock tube experiments and modeling of homogenous ignition process, two-stage heat release was also observed by Mathieu et al. [6] and Nauclér et al. [7]. Besides, a double cellular structure was observed in the detonation experiments for gaseous nitromethane/oxygen mixtures [8]. Sturtzer et al. [9] calculated the 1D ZND detonation structure using a detailed mechanism for nitromethane. They found that heat is released in two main successive reaction steps characterized by their own induction length, which justifies the existence of a two-level detonation cellular structure [9].

Though the two or three step heat release in nitromethane combustion was identified in previous studies listed above, the chemical reactions responsible for the multi-stage heat release in nitromethane/air flames are still not well known. This motivates the present work, whose first objective is to investigate the two-stage heat release and the corresponding reactions in premixed, planar nitromethane/air flames. The influence of equivalence ratio, initial pressure and initial temperature on the two-stage heat release in nitromethane/air flames is also investigated.

Laminar flame speed is popularly used to validate and develop the chemical mechanism of different fuels [10,11]. Due to its simple configuration and well-defined stretch rate, the propagating spherical flame method is popularly used to measure the

* Corresponding author.: Tel.: +86-10-62766232
E-mail addresses: cz@pku.edu.cn, chenzheng@coe.pku.edu.cn (Z. Chen).

http://dx.doi.org/10.1016/j.combustflame.2017.05.013
0010-2180/

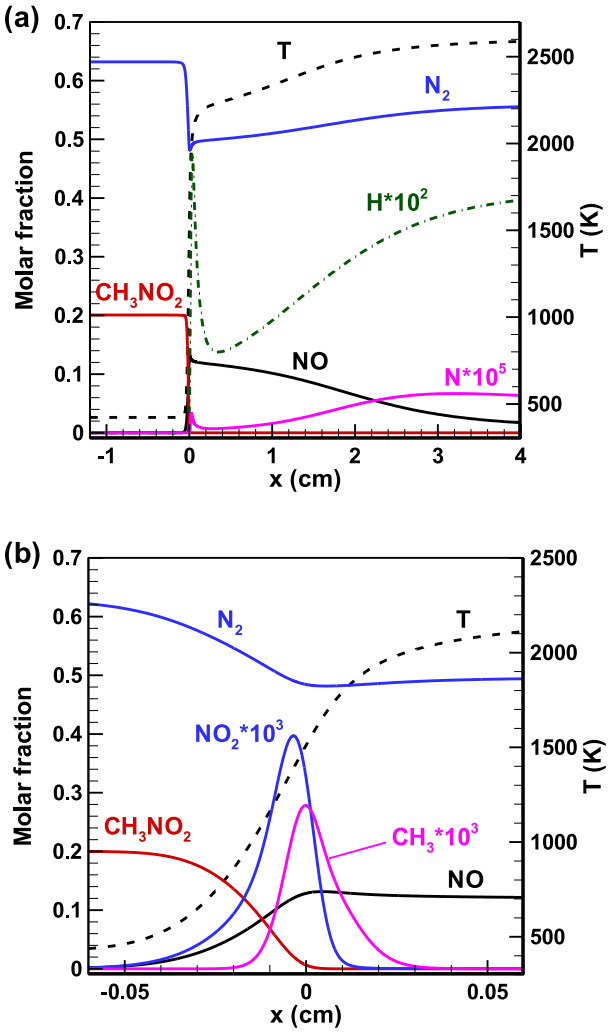

Fig. 1. Distributions of temperature and molar fraction of different species in premixed nitromethane/air flame with $\phi=0.9$, $T_u = 423$ K and $P=1$ atm and (b) magnifies the results corresponding to the first stage heat release around $x=0$ cm.

laminar flame speed, especially at high pressures [12–14]. For nitromethane/air mixture, Brequigny et al. [15] measured laminar flame speed from propagating spherical flames at different initial pressures and equivalence ratios. However, Nauclér et al. [5] pointed out that it is difficult to accurately measure the laminar flame speed from propagating spherical nitromethane/air flames due to the two-stage heat release and large flame thickness. Currently, it is not clear how and why the two-stage heat release affects the laminar flame speed measurement of nitromethane/air from propagating spherical flames. Therefore, the second objective of the present study is to answer this question by studying propagating spherical flames in nitromethane/air mixtures.

Both 1D planar and 1D spherical premixed nitromethane/air flames are considered in this study. Using the planar flame, we shall investigate the characteristics of the two-stage heat release and the chemical reactions involved in these two stages. Using the spherical flame, we shall explain how the two-stage heat release affects the laminar flame speed determination. For both planar and spherical flames, the effects of equivalence ratio, initial pressure and initial temperature are examined.

2. Numerical methods

As mentioned before, two 1D premixed flame configurations are considered in this study: one is the unstretched freely-propagating planar flame and the other is the positively-stretched propagating spherical flame. The PREMIX code [16] was used to simulate the planar flame and to get the flame structure and unstretched laminar flame speed. Thermal diffusion and multicomponent molecular transport model were included in all simulations. The number of grid points was always kept to be above 1000 so that the flame structure was well resolved and the results were grid independent. Since nitromethane/air flame with two-stage heat release has very large flame thickness, a large domain size of 50 cm was used in simulation.

The propagating spherical flame was simulated using the in-house code A-SURF [17–19]. A-SURF solves the conservation equations for compressible, multicomponent, reactive flow in a spherical coordinate by the finite volume method. The CHEMKIN package [20] was incorporated into A-SURF to calculate the thermodynamic properties, transport properties and reaction rates. A-SURF was successfully used in previous studies on flame and detonation propagation [13,21–28]. The readers are referred to Refs. [17–19] for details on numerical schemes and code validation of A-SURF. Dynamic adaptive mesh was used to accurately resolve the propagating spherical flame front, which were always fully covered by the finest mesh with the size of 8 μm. To avoid confinement effect [17,29], a large chamber radius of $R_w = 50$ cm was used in all simulations. As summarized in Ref. [13], there are different factors affecting the accurate measurement of laminar flame speed from propagating spherical flames. In the present study, we focused on the influence of two-stage heat release and thereby other factors such as radiation, flame instability and nonlinear stretch behavior were not considered.

In the literature, there are several chemical mechanisms for CH_3NO_2 [6,15,30–32] and NO_2 ([40] and references therein). Since the mechanism of Brequigny et al. [15] containing 88 species and 701 reactions was validated against the laminar flame speed data of CH_3NO_2 at $T_u = 423$ K, $P=0.5\sim3.0$ bar and $\phi=0.5\sim1.3$ and it yields reasonably well prediction, it was used in all simulations in this study.

Two global reactions for nitromethane/air combustion were proposed in the literature [31,33]:

$$CH_3NO_2+0.75(O_2+3.78N_2)= CO_2+1.5H_2O + 3.32N_2 \quad (1)$$

$$CH_3NO_2+1.25(O_2+3.78N_2)= CO_2+1.5H_2O + NO + 4.7N_2 \quad (2)$$

Both global reactions have been used recently [5,6,15]. In Eq. (1), N_2 is the only product containing nitrogen atom [15], while Eq. (2) indicates that NO is a stable product [5]. According to the results to be presented in this study, neither Eq. (1) nor Eq. (2) is unanimously accurate: in fuel-lean nitromethane/air flames, NO is a stable product; while for rich flames NO is converted into N_2. Nevertheless, the equivalence ratios according to Eqs. (1) and (2) have a linear relationship of $\phi_{Eq.\,(1)}=0.6\phi_{Eq.\,(2)}$ and thereby they can be directly converted into each other. Since the only experimental study on propagating spherical flames in nitromethane/air was conducted by Brequigny et al. [15] in which Eq. (1) was used, we also used Eq. (1) in this study. Note that similar to Brequigny et al. [15], we considered the synthetic air with 79.1% N_2 and 20.9% O_2 and thereby the molar ratio of N_2 to O_2 is 3.78 in Eqs. (1) and (2).

3. Two-stage heat release in premixed planar nitromethane/air flame

We first investigated the two-stage heat release in premixed planar nitromethane/air flames.

Figure 1 shows the flame structure of premixed nitromethane/air with $\phi=0.9$, $T_u = 423$ K and $P=1$ atm. The temperature profile indicates that there are two-stage heat release: the first stage

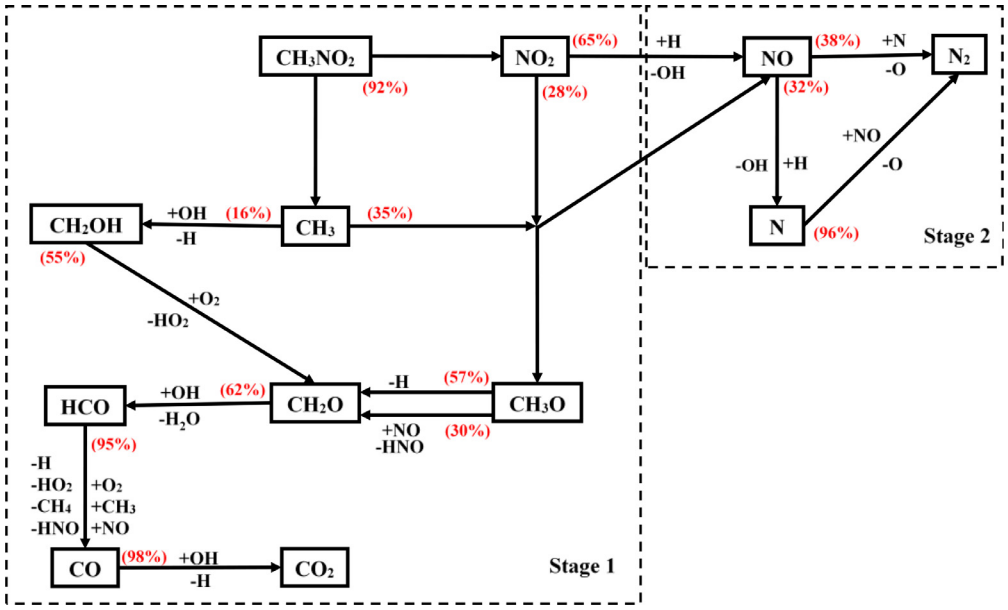

Fig. 2. Main reaction pathways involved in nitromethane oxidation for premixed planar nitromethane/air flame at $\phi=0.9$, $T_u = 423$ K and $P=1$ atm. The red number in parenthesis shows the percentage of consumption rate through the specific pathway. (For interpretation of the references to color in this figure legend, the reader is referred to the web version of this article.)

corresponding to the sharp temperature increase around $x=0$ cm; and the second stage corresponding to the gradually temperature increase within $0 < x < 3$ cm. Figure 1(b) shows that the main temperature increase (from $T_u = 423$ K to $T \approx 2200$ K) is caused by the first stage heat release, during which CH_3NO_2 is consumed, NO_2 and CH_3 are intermediate species, and NO is produced. Therefore, the global reaction for the first stage heat release can be described by Eq. (2). It is noted that the decrease of N_2 molar fraction shown in Fig. 1(b) is not due to the consumption of N_2. It is due to the global reaction in Eq. (2) results in an increase in the total number of moles. Figure 1(a) shows that the second stage heat release induces relative small temperature increase (from $T \approx 2200$ K to $T \approx 2600$ K). During the second stage heat release, NO is slowly converted into N_2 through reaction N+NO=N_2 +O, for which the N atom is mainly produced through slow reaction NO+H=N+OH.

In order to identify the chemical reactions responsible for the two-stage heat release, we conducted reaction pathway analysis for nitromethane/air flame at $\phi=0.9$, $T_u = 423$ K and $P=1$ atm. The results are shown in Fig. 2. For each species, the percentage of consumption rate through specific reaction is indicated by the number in parenthesis. It is observed that 92% of nitromethane dissociates into CH_3 and NO_2 through reaction $CH_3NO_2(+M)=CH_3+NO_2(+M)$. The first stage heat release is mainly induced by NO_2 consumption and NO production through reactions $NO_2+H=NO+OH$ and $CH_3+NO_2=CH_3O+NO$. During the first stage heat release, the oxidation pathway for CH_3 is shown to follow $CH_3 \rightarrow CH_2O \rightarrow HCO \rightarrow CO \rightarrow CO_2$. Similar observation was made in [15]. During the second stage heat release, NO is mainly converted into N_2 through reactions N+NO=N_2 +O, and the reverse reaction of N+OH=NO+H. The simulation results indicate that the reverse reaction of R387 (i.e., NO+H→N+OH) has low reaction rate, and thereby the second stage heat release is much longer than the first stage heat release. As will be discussed later, the low reaction rate of R387 is mainly due to the low concentration of H atom during the second stage heat release.

To further demonstrate the key reactions involved in the second stage heat release, two mechanisms, Mech-1 and Mech-2, were obtained by deleting some elementary reactions listed in Table 1 from the original mechanism (detonated as Mech-0). The results

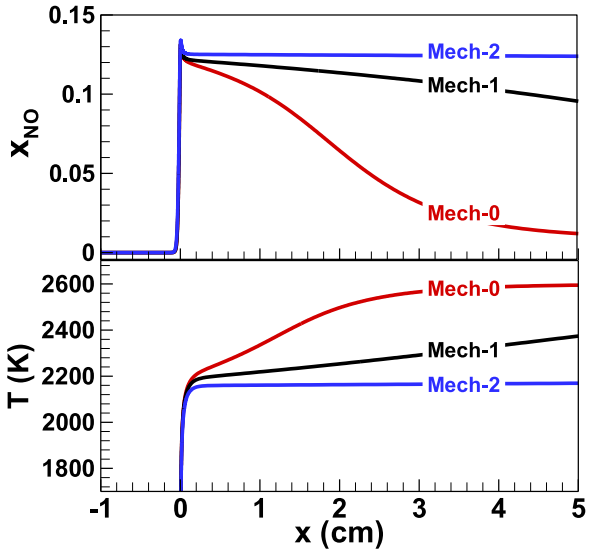

Fig. 3. Distributions of NO molar fraction and temperature in nitromethane/air flame with $\phi=0.9$, $T_u = 423$ K and $P=1$ atm. The results from three mechanisms listed in Table 1 are shown together for comparison.

predicted by these three mechanisms are compared in Fig. 3. Comparison between results from Mech-0 and Mech-1 indicates that the second stage heat release and NO consumption are mainly due to the reverse of R387, i.e., NO+H→N+OH. However, the second stage heat release is not completely forbidden by deleting R387. The results for Mech-2 indicate that the second stage heat release disappears only when the six reactions R346, R375, R376, R387, R388 and R389 listed in Table 1 are all deleted. Therefore, the second stage heat release is mainly caused by R387 and it is also contributed by five other reactions: R346, R375, R376, R388 and R389. Davidenko et al. [39] found that the second stage heat release merges with the first one after artificially setting the activation energy of NO+H→N+OH to be zero (i.e., to greatly increase the reaction rate of this reaction much faster). Their observation is consistent with our results mentioned above.

Table 1
Different versions of chemical mechanism based on the one of Brequigny et al. [15].

Version	Reactions that are deleted		
Mech-0	Non (the original mechanism)		
Mech-1	R387: N+OH=NO+H		
Mech-2	R346: N_2O+O=NO+NO	R375: NH+O=NO+H	R376: NH+OH=HNO+H
	R387: N+OH=NO+H R	R388: N+O_2 =NO+O	R389: N+NO=N_2 +O

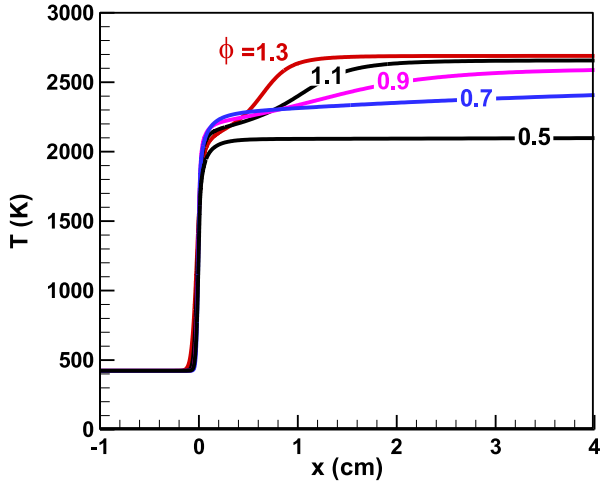

Fig. 4. Temperature profiles of premixed nitromethane/air flames at T_u = 423 K, P=1 atm and different equivalence ratios. The original mechanism (Mech-0) is used in simulation.

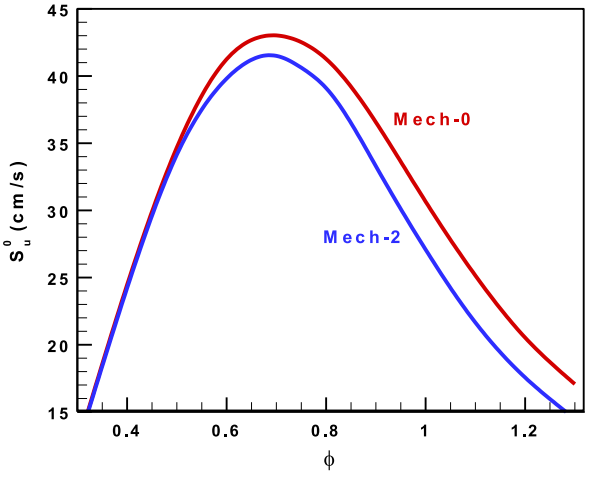

Fig. 5. Laminar flame speed of nitromethane/air at T_u = 423 K and P=1 atm.

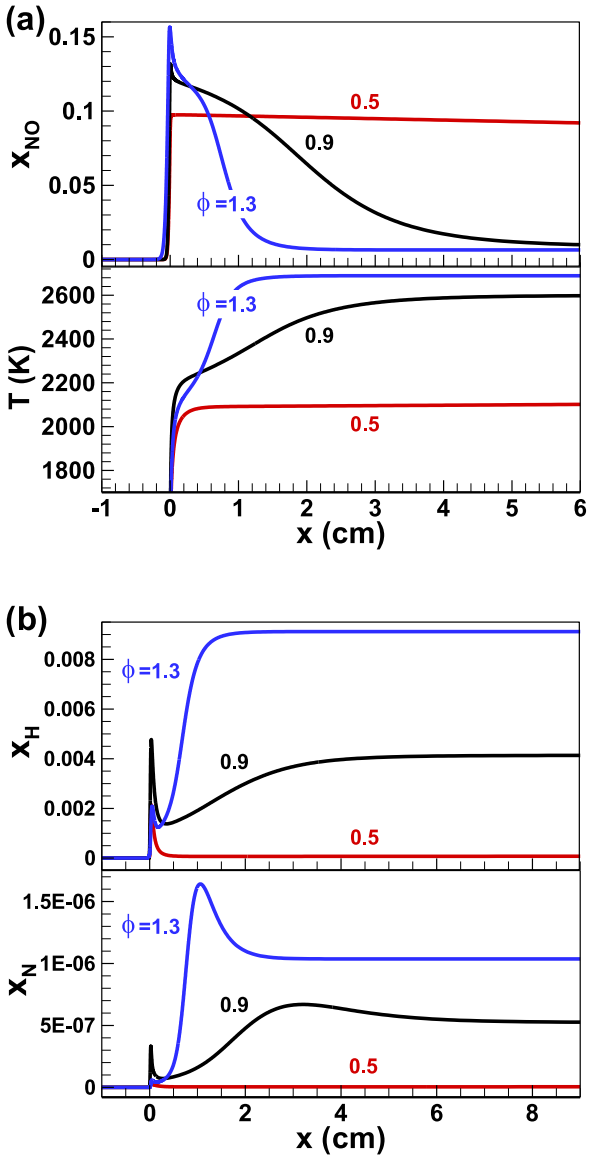

Fig. 6. Distributions of temperature and molar fractions of NO, H and N in nitromethane/air flame with T_u = 423 K, P=1 atm and different equivalence ratios.

Figure 4 compares the temperature distributions of nitromethane/air flames with different equivalence ratios. For the very lean case of ϕ=0.5, the temperature profile indicates that there is only one stage heat release, for which the main reaction pathways are those for stage 1 shown in Fig. 2. With the increase of the equivalence ratio, the second stage heat release occurs. It is noted that the flame temperature after the first stage heat release (i.e., temperature around x=0 cm) becomes the highest for ϕ=0.7, though the mixture with ϕ=1.3 has the highest flame temperature after the second stage heat release. In [5,15] the maximum laminar flame speed was found to occur for the equivalence ratio around 0.75. This was confirmed by Fig. 5, which shows the laminar flame speed predicted by Mech-0 and Mech-2, respectively, with and without forbidding the second stage heat release. At low equivalence ratio (ϕ < 0.5), the laminar flame speed predicted by Mech-0 is close to that by Mech-2 since only one stage heat release occurs for very lean case as shown in Fig. 4. Figure 5 indicates that the second stage heat release helps to enlarge the laminar flame speed though it is mainly determined by the first stage heat release.

To further assess the influence of equivalence ratio on the second stage heat release, the temperature and NO, H and N molar fraction distributions for ϕ=0.5, 0.9 and 1.3 are compared in Fig. 6. It is seen while NO is not consumed and remains as a stable product for ϕ=0.5, it is consumed completely for ϕ=0.9 and 1.3. Therefore, Eq. (2) accurately defines the global reaction of nitromethane/air at ϕ=0.5, while Eq. (1) should be used for ϕ=0.9 and 1.1. Moreover, the NO consumption rate for ϕ=1.3 is

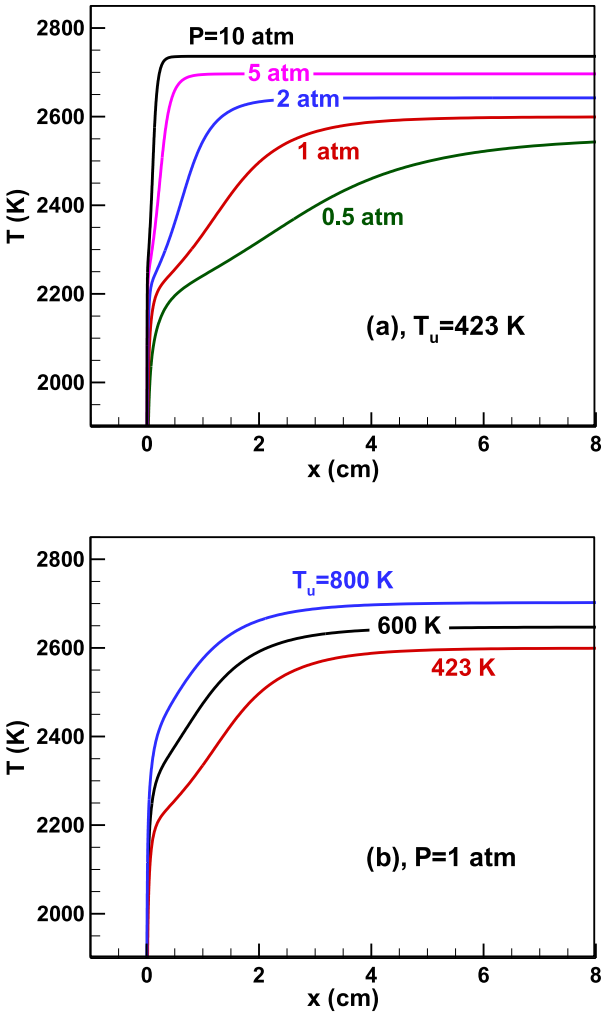

Fig. 7. Effects of initial pressure (a) and initial temperature (b) on the temperature profile of premixed nitromethane/air flame with $\phi = 0.9$.

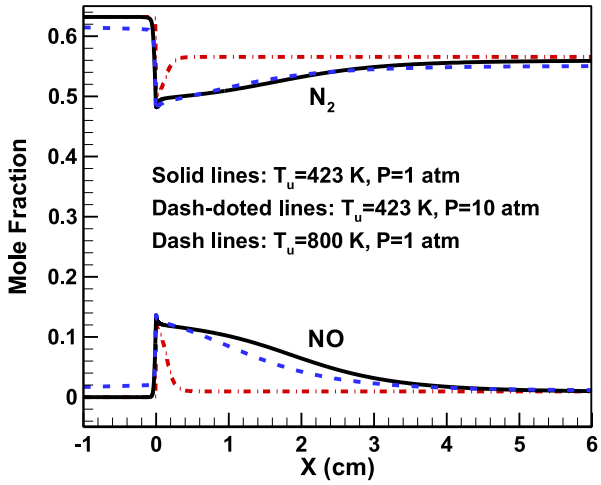

Fig. 8. Distributions of N_2 and NO molar fractions in nitromethane/air flame with $\phi = 0.9$.

much faster than that for $\phi = 0.9$, which explains why the flame is much thicker at $\phi = 0.9$. As mentioned before, the second stage heat release is mainly caused by the reverse reaction of R387, i.e., NO+H→N+OH. As shown in Fig. 6(b), for $\phi = 0.5$ there is little H atom after the main reaction zone around $x = 0$ cm and thereby the second stage heat release does not occur. Besides, the production rate of H for $\phi = 0.9$ is much smaller than that for $\phi = 1.3$. This causes lower reaction rate of R387 for $\phi = 0.9$ and consequently increases the length of second stage heat release as shown in Fig. 6.

The above results are only for $T_u = 423$ K and $P = 1$ atm. Besides the equivalence ratio, the initial pressure and temperature also affect the second stage heat release. The influence of initial pressure and temperature on the temperature profile of premixed nitromethane/air flame with $\phi = 0.9$ are demonstrated in Fig. 7. According to Fig. 7(a), the temperature increment occurs faster and the flame thickness becomes smaller at higher pressure. However, Fig. 7(b) shows that the thickness of the second stage heat release only slightly reduces as the initial temperature increases from 423 K to 800 K. The influence of the initial pressure and temperature on the second stage heat release is further demonstrated in Fig. 8, which compares the distributions of NO and N_2 molar fraction. It is observed that during the second stage heat release, NO consumption and N_2 production become much faster at higher pressure of $P = 10$ atm while they are changed slightly at higher initial temperature of $T_u = 800$ K. Therefore, the second stage heat release is strongly affected by the initial pressure while the initial temperature has little influence.

4. Impact of two-stage heat release on laminar flame speed measurement

In this section we considered spherical flame propagation in nitromethane/air mixture and investigated the impact of two-stage heat release on the determination of laminar flame speed.

Figure 9 shows the temporal evolution of temperature and flow speed distributions for spherical nitromethane/air flame at $\phi = 0.9$, $T_u = 423$ K and $P = 1$ atm. The results predicted by two mechanisms, Mech-0 and Mech-2, were plotted together for comparison. As mentioned before and indicated by the temperature distributions shown in Fig. 9(a), two-stage heat release occurs for the results predicted by Mech-0; while there is only single-stage heat release for Mech-2. The second stage heat release after the main flame front induces further thermal expansion and thereby the burned gas is shown to have positive flow speed in Fig. 9(b). When the second stage heat release is terminated as in Mech-2, the burned gas is shown to be static. Therefore, the second stage heat release induces non-zero flow in burned gas.

As found in previous studies [13,17,29,34], non-static burned gas, which can also be induced by radiation and compression, has great impact on the accuracy of laminar flame speed measurement from propagating spherical flames. In outwardly propagating spherical flames, the laminar flame speed relative to burned gas is $S_b = S - u_b$, where $S = dR_f/dt$ is the flame propagation speed and u_b is the flow speed of burned gas close to the reaction front. Usually only the flame front history $R_f = R_f(t)$ is recorded and it is difficult to measure the flow speed of burned gas in experiments [35,36]. Consequently, the flame propagation speed is usually considered as the laminar flame speed relative to burned gas (i.e., $S_b \approx S$), and the accuracy of laminar flame speed measurement depends on the magnitude of burned gas speed, i.e., $|u_b|$. Therefore, the second stage heat release affects the determination of laminar flame speed through non-zero burned gas speed.

Figure 10 shows the change of flame propagation speed S with stretch rate K, which is $K = 2S/R_f$ for propagating spherical flame. When the second stage heat release is terminated as in Mech-2, S changes linearly with K and the unstretched flame speed can be obtained from linear extrapolation. However, when the two-stage heat release appears as in Mech-0, S does not change linearly with K. It is observed that linear extrapolation II based on $1 \le R_f \le 2$ cm

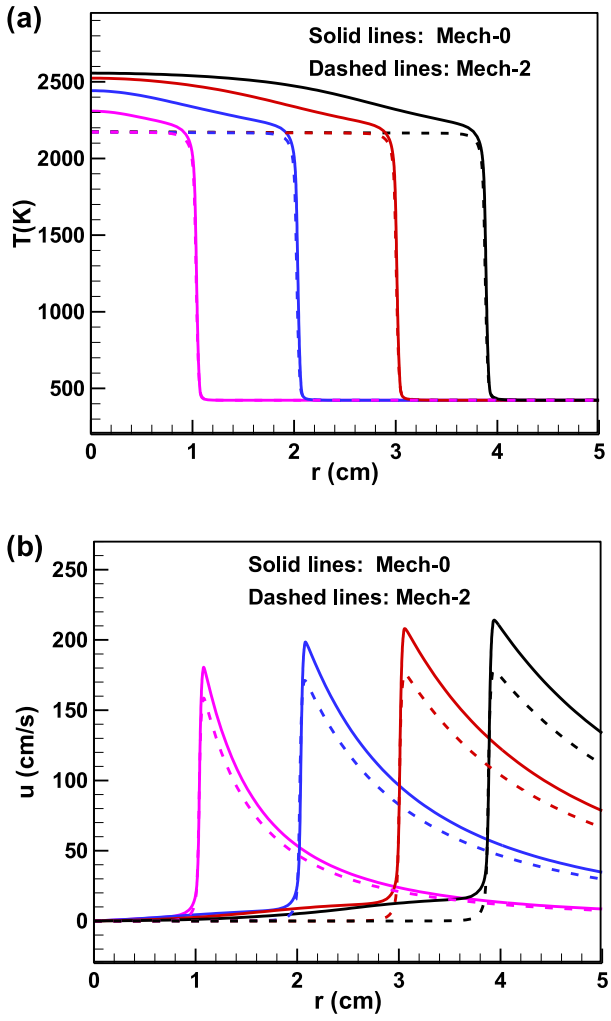

Fig. 9. The evolution of temperature (a) and flow speed (b) distributions for spherical nitromethane/air flame at $\phi = 0.9$, $T_u = 423$ K and $P = 1$ atm.

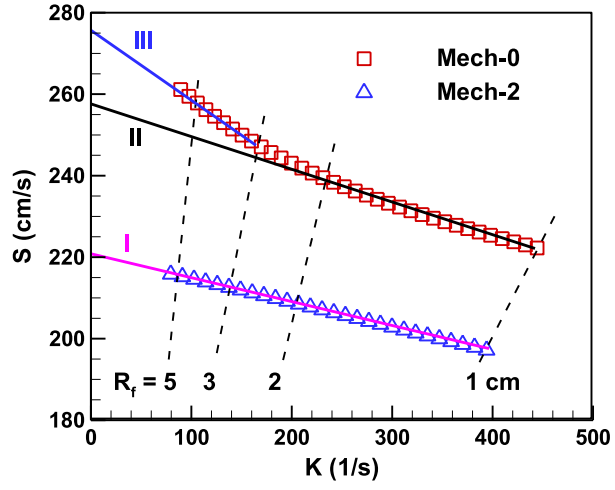

Fig. 10. Flame propagation speed as a function of stretch rate for spherical nitromethane/air at $\phi = 0.9$, $T_u = 423$ K and $P = 1$ atm. The symbols denote simulation results using two mechanisms. The solid lines stand for linear fitting and the dashed lines denote the flame radii contours (they are straight lines since $R_f = 2S/K$).

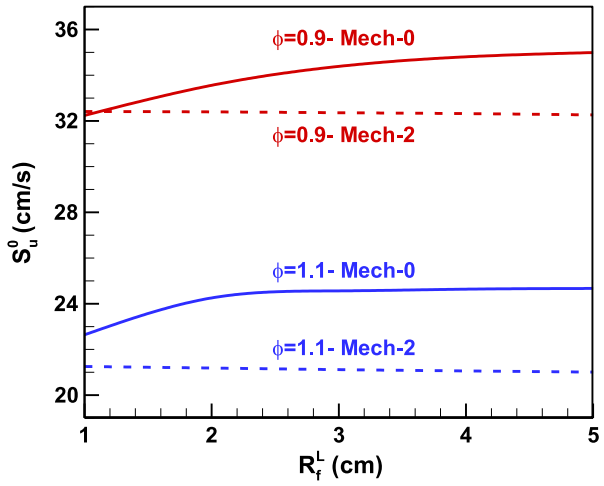

Fig. 11. Laminar flame speed from linear extrapolation based on different flame radius ranges of $[R_f^L,\ R_f^L + 1\ \text{cm}]$ for nitromethane/air flames at $T_u = 423$ K and $P = 1$ atm.

Table 2
Different methods used to calculate unstretched laminar flame speed from propagating spherical flames. S_b and S_u are respectively the stretched laminar flame speed with respect to burned and unburned gas. L_b and L_u are, respectively, the Markstein length with respect to burned and unburned gas. S_b^0 and S_u^0 are unstretched laminar flame speed with respect to burned and unburned gas, respectively. σ^{eq}, σ^{center} and σ^{flame} are density ratios defined in the text.

Method	Equations		
I	$S_b = dR_f/dt$,	$S_b = S_b^0 - L_b K$,	$S_u^0 = \sigma^{eq} S_b^0$
II	$S_b = dR_f/dt$,,	$S_b = S_b^0 - L_b K$	$S_u^0 = \sigma^{center} S_b^0$
III	$S_b = dR_f/dt - u_b$,	$S_b = S_b^0 - L_b K$,	$S_u^0 = \sigma^{flame} S_b^0$
IV	$S_u = dR_f/dt - u_u$,	$S_u = S_u^0 - L_u K$	

yields different result from linear extrapolation III based on $3 \le R_f \le 5$ cm. Therefore, the unstretched laminar flame speed is sensitive to the flame radius range used in linear extrapolation when there is two-stage heat release.

This is further demonstrated by Fig. 11, in which the laminar flame speeds from linear extrapolation based on different flame radius ranges are depicted. The laminar flame speed S_u° was obtained through multiplying S_b° from linear extrapolation by the density ratio between burned gas (at equilibrium condition) and unburned gas σ^{eq}, i.e., $S_u^0 = \sigma^{eq} S_b^0$. For Mech-2 without two-stage heat release, flame radius range has little effect on the extrapolated laminar flame speed. However, when two-stage hear release occurs as for Mech-0, the results are sensitive to the flame radius range used in linear extrapolation: S_u° extrapolated from the range of $1 \le R_f \le 2$ cm is 32.2 cm/s and 22.6 cm/s for $\phi = 0.9$ and $\phi = 1.1$, respectively; while that from the range of $5 \le R_f \le 6$ cm is 35.0 cm/s and 24.7 cm/s for $\phi = 0.9$ and $\phi = 1.1$, respectively. In order to diminish the confinement effect [17,29], the flame radius range used in experiments is usually close to $1 \le R_f \le 2$ cm (e.g., [15]). Therefore, Fig. 11 indicates the error in laminar flame speed measured by Brequigny et al. [15] can exceed 8% due to the non-zero burned gas speed induced by two-stage heat release.

Table 2 lists four methods to determine S_u^0. Method I is popularly used and it was used by Brequigny et al. [15]. It works well for mixtures with single stage heat release and with effective Lewis number close to unity [13]. However, as mentioned before, method I does not work well for nitromethane/air since the two-stage heat release induces positive burned gas speed which should not be neglected. Instead of using the density ratio at equilibrium condition,

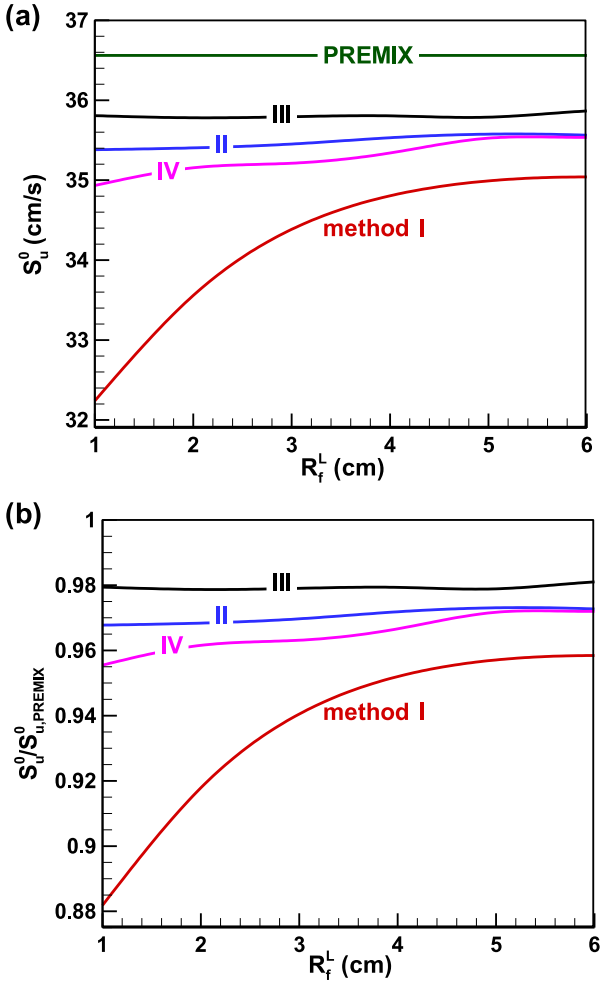

Fig. 12. Laminar flame speed (a) and normalized laminar flame speed (b) extrapolation based on different flame radius ranges of [R_f^L, R_f^L+ 1 cm] for nitromethane/air flames at $\phi = 0.9$, $T_u = 423$ K and $P = 1$ atm.

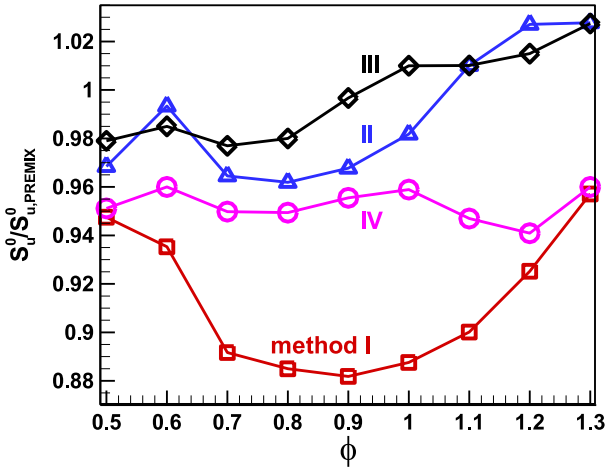

Fig. 13. Effects of different methods on the laminar flame speed measurement for nitromethane/air at $T_u = 423$ K and $P = 1$. The flame radius range used in extrapolation is $1 \le R_f \le 2$ cm.

in method II we use the density ratio between burned gas at the center (i.e., $r = 0$) and unburned gas, σ^{center}. The burned gas speed and the burned gas density at the center are related through the continuity equation. As shall be demonstrated, using this density ratio σ^{center} helps to reduce the error induced by neglecting the positive burned gas speed. In method III, the burned gas speed, u_b, is included and σ^{flame} is the density ratio between burned gas near the flame front and unburned gas. Noted that it is difficult to get σ^{center}, u_b and σ^{flame} in experiments though they are readily available in the present simulation. In Method IV, the density ratio is not used and the stretched flame speed relative to unburned gas is obtained through simultaneous measurement of flame front history and flow speed of unburned gas (using both high-speed Schlieren and particle image velocimetry method) [35–38] In simulation, the flow speed of unburned gas, u_u, is obtained from extrapolating the unburned gas speed to the location of the flame front. For Method IV, both dR_f/dt and u_u are much larger that S_u. Therefore, the uncertainty in the measurement of u_u can greatly affect the accuracy of laminar flame speed measurement.

Figure 12 compares the laminar flame speeds obtained from different methods. The results from PREMIX are shown together for comparison. As expected, method I is shown to greatly underpredict laminar flame speed, especially for extrapolation based on small flames with $1 \le R_f \le 2$ cm. Unlike method I, methods II, III and IV make the extrapolation results nearly independent of flame radius range and close to those predicted by PREMIX. Therefore, using method II, III or IV helps to increase the accuracy in laminar flame speed measurement for nitromethane. This is further demonstrated by results at different equivalence ratios (see Fig. 13) and different initial pressures and temperatures (see Fig. 14).

Since method II is much more accurate than method I, it can be used to correct the experimental data reported by Brequigny et al. [15]. The only difference between methods I and II is that different density ratios, σ^{eq} and σ^{center}, are used. Figure 15 compares these two density ratios. The difference is shown to increase with the equivalence ratio. This is because the two-stage heat release becomes stronger at larger equivalence ratio as shown in Fig. 4. The density ratio σ^{center} from the present simulation was used to correct the laminar flame speeds measured in [15] and the results are shown in Fig. 16. After the correction the laminar flame speeds become larger since $\sigma^{center} > \sigma^{eq}$ as shown in Fig. 15. Besides, Fig. 16(a) shows that the corrected values agree well with those predicted by the power law expression of Nauclér et al. [5]. It is noted that the flat flame experiments were originally performed for $T_u = 338$ K, 348 K and 358 K and the power law was used to extrapolate the laminar flame speeds at $Tu = 423$ K [5]. According to [5], the extrapolated laminar flame speed at $T_u = 423$ K induced ± 1.5–2 cm/s uncertainty in reported results.

5. Conclusions

Numerical simulations considering detailed chemistry and transport were conducted for premixed nitromethane/air flames. The two-stage heat release and its influence on laminar flame speed measurement were investigated for nitromethane/air mixtures at different equivalence ratios, initial pressures and initial temperatures. The main conclusions are:

1. For premixed planar nitromethane/air flame, the occurrence of two-stage heat release strongly depends on the equivalence ratio and single-stage heat release occurs for very fuel-lean mixture. During the second stage heat release, NO is slowly converted into N_2. Therefore, the global reaction for nitromethane/air combustion is described by Eqs. (1) and (2), respectively for cases with and without the second stage heat release. Comparison between predictions from different mechanisms demonstrates that the second stage heat release is mainly caused by the reaction of NO+H→N+OH. With the increase of the initial pressure, the reaction zone length of the second stage heat release is greatly reduced. Compared to the

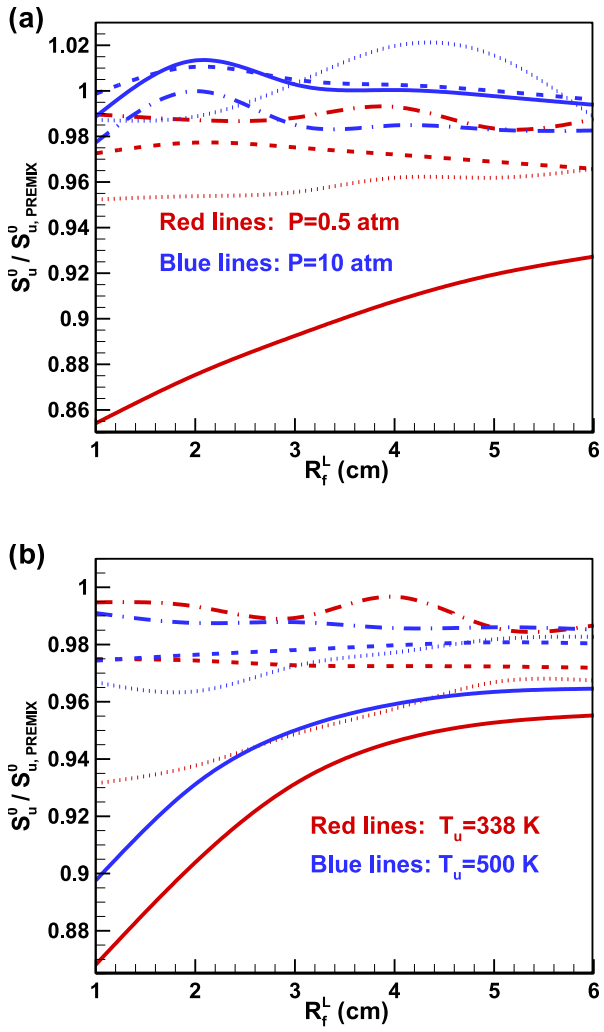

Fig. 14. Normalized laminar flame speed extrapolated using different flame radius ranges of [R_f^L, R_f^L+ 1 cm] for nitromethane/air flames at (a) ϕ=0.9, T_u=423 K and different pressures; and (b) ϕ=0.9, P=1 atm and different initial temperatures. $S_u{}^0{}_{,PREMIX}$ is the laminar flame speed calculated from PREMIX. Solid lines for method I, dashed lines for method II, dash-dotted lines for method III and dotted lines for method IV. (For interpretation of the references to color in this figure legend, the reader is referred to the web version of this article.)

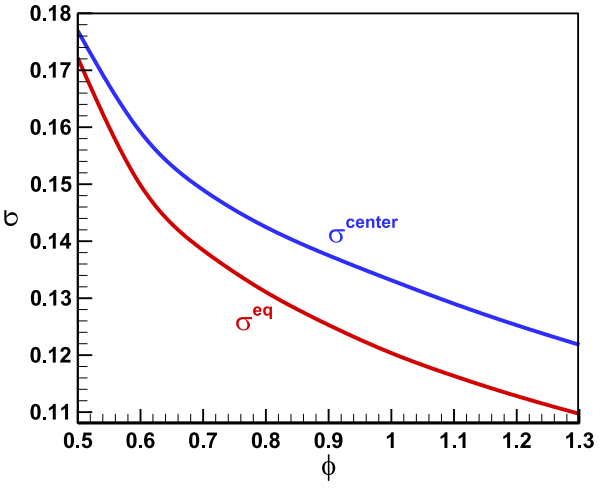

Fig. 15. Density ratio for nitromethane/air at T_u = 423 K and P=1 atm.

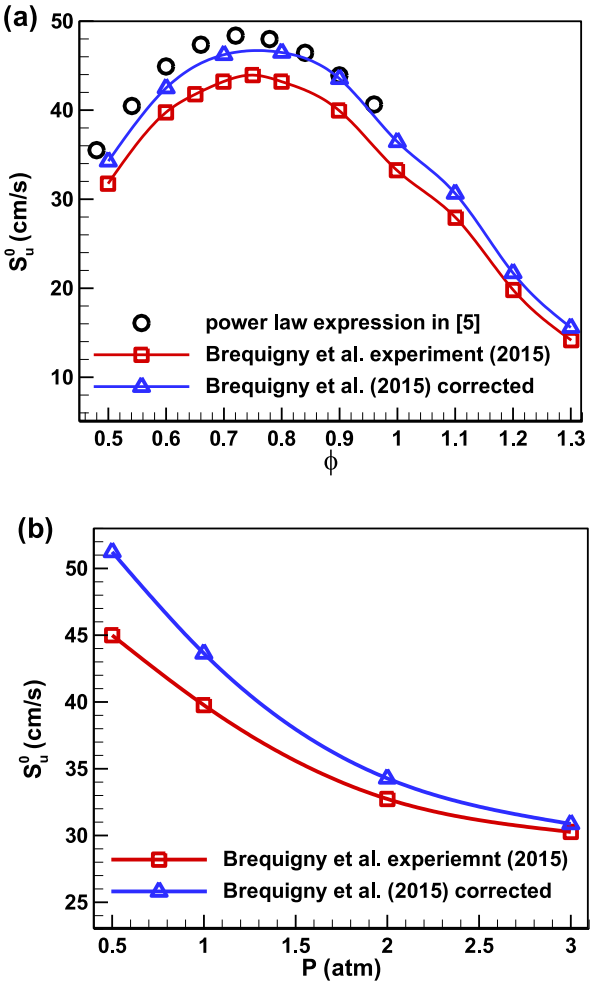

Fig. 16. Laminar flame speeds of nitromethane/air: (a), at T_u = 423 K, P=1 atm and different equivalence ratios; and (b) at ϕ=0.9 and T_u = 423 K and different pressures.

initial pressure, the initial temperature has much smaller influence on the reaction zone length of the second stage heat release.

2. For premixed spherical nitromethane/air flame, the second stage heat release induces positive burned gas speed and thereby it affects the laminar flame speed measurement of nitromethane/air from propagating spherical flames. When there is two-stage heat release, the unstretched laminar flame speed is very sensitive to the flame radius range used in linear extrapolation. Traditional method neglecting burned gas speed and using the density ratio at equilibrium condition can greatly under-predict the laminar flame speed of nitromethane/air, especially for extrapolation based on small flames with 1 $\leq R_f \leq$ 2 cm. The experimental data reported by Brequigny et al. [15] were corrected by using the density ratio between burned gas at the center and unburned gas. Compared to the original data, the corrected results were shown to have better agreement with those predicted by the power law expression based on experimental data of flat flames by Nauclér et al. [5].

Acknowledgments

This work was supported by National Natural Science Foundation of China (Nos. 51322602 and 91541204). We thank Dr. Zhen-yu Tian (at Institute of Engineering Thermophysics, Chinese Academy

of Sciences) for helpful discussion on the chemical kinetics of nitromethane.

References

[1] R.F. Cracknell, J.C.G. Andrae, L.J. McAllister, M. Norton, H.L. Walmsley, The chemical origin of octane sensitivity in gasoline fuels containing nitroalkanes, Combust. Flame 156 (2009) 1046–1052.

[2] T. Litzinger, M. Colket, M. Kahandawala, S.Y. Lee, D. Liscinsky, K. McNesby, R. Pawlik, M. Roquemore, R. Santoro, S. Sidhu, S. Stouffer, Fuel additive effects on soot across a suite of laboratory devices, part 2: nitroalkanes, Combust. Sci. Technol. 183 (2011) 739–754.

[3] E. Boyer, K.K. Kuo, Modeling of nitromethane flame structure and burning behavior, Proc. Combust. Inst. 31 (2007) 2045–2053.

[4] A.R. Hall, H.G. Wolfhard, Multiple reaction zones in low pressure flames with ethyl and methyl nitrate, methyl nitrite and nitromethane, Symp. Int. Combust. 6 (1957) 190–199.

[5] J.D. Nauclér, E.J.K. Nilsson, A.A. Konnov, Laminar burning velocity of nitromethane + air flames: a comparison of flat and spherical flames, Combust. Flame 162 (2015) 3803–3809.

[6] O. Mathieu, B. Giri, A.R. Agard, T.N. Adams, J.D. Mertens, E.L. Petersen, Nitromethane ignition behind reflected shock waves: experimental and numerical study, Fuel 182 (2016) 597–612.

[7] J.D. Nauclér, Y. Li, E.J.K. Nilsson, H.J. Curran, A.A. Konnov, An experimental and modeling study of nitromethane + O_2 + N_2 ignition in a shock tube, Fuel 186 (2016) 629–638.

[8] H.N. Presles, D. Desbordes, M. Guirard, C. Guerraud, Gaseous nitromethane and nitromethane-oxygen mixtures: a new detonation structure, Shock Waves 6 (1996) 111–114.

[9] M.-O. Sturtzer, N. Lamoureux, C. Matignon, D. Desbordes, H.-N. Presles, On the origin of the double cellular structure of the detonation in gaseous nitromethane and its mixtures with oxygen, Shock Waves 14 (2005) 45–51.

[10] C.K. Law, C.J. Sung, H. Wang, T.F. Lu, Development of comprehensive detailed and reduced reaction mechanisms for combustion modeling, AIAA J. 41 (2003) 1629–1646.

[11] E. Ranzi, A. Frassoldati, R. Grana, A. Cuoci, T. Faravelli, A.P. Kelley, C.K. Law, Hierarchical and comparative kinetic modeling of laminar flame speeds of hydrocarbon and oxygenated fuels, Prog. Energy Combust. Sci. 38 (2012) 468–501.

[12] F.N. Egolfopoulos, N. Hansen, Y. Ju, K. Kohse-Höinghaus, C.K. Law, F. Qi, Advances and challenges in laminar flame experiments and implications for combustion chemistry, Prog. Energy Combust. Sci. 43 (2014) 36–67.

[13] Z. Chen, On the accuracy of laminar flame speeds measured from outwardly propagating spherical flames: methane/air at normal temperature and pressure, Combust. Flame 162 (2015) 2442–2453.

[14] M. Faghih, Z. Chen, The constant-volume propagating spherical flame method for laminar flame speed measurement, Sci. Bull. 61 (2016) 1296–1310.

[15] P. Brequigny, G. Dayma, F. Halter, C. Mounaïm-Rousselle, T. Dubois, P. Dagaut, Laminar burning velocities of premixed nitromethane/air flames: an experimental and kinetic modeling study, Proc. Combust. Inst. 35 (2015) 703–710.

[16] R.J. Kee, J. Grcar, M. Smooke, J. Miller, PREMIX: a FORTRAN program for modeling steady laminar one-dimensional premixed flames, 1985 Sandia National Laboratory, SAND85-8240.

[17] Z. Chen, Effects of radiation and compression on propagating spherical flames of methane/air mixtures near the lean flammability limit, Combust. Flame 157 (2010) 2267–2276.

[18] Z. Chen, M.P. Burke, Y.G. Ju, Effects of Lewis number and ignition energy on the determination of laminar flame speed using propagating spherical flames, Proc. Combust. Inst. 32 (2009) 1253–1260.

[19] P. Dai, Z. Chen, Supersonic reaction front propagation initiated by a hot spot in n-heptane/air mixture with multistage ignition, Combust. Flame 162 (2015) 4183–4193.

[20] R.J. Kee, F. Rupley, J. Miller, CHEMKIN-II: A FORTRAN chemical kinetics package for the analysis of gas-phase chemical kinetics, 1993 Sandia National Laboratory, SAND89-8009B.

[21] Z. Chen, M.P. Burke, Y. Ju, On the critical flame radius and minimum ignition energy for spherical flame initiation, Proc. Combust. Inst. 33 (2011) 1219–1226.

[22] W. Zhang, Z. Chen, W. Kong, Effects of diluents on the ignition of premixed H_2/air mixtures, Combust. Flame 159 (2012) 151–160.

[23] H. Zhang, P. Guo, Z. Chen, Critical condition for the ignition of reactant mixture by radical deposition, Proc. Combust. Inst. 34 (2013) 3267–3275.

[24] H. Yu, Z. Chen, End-gas autoignition and detonation development in a closed chamber, Combust. Flame 162 (2015) 4102–4111.

[25] P. Dai, Z. Chen, S. Chen, Y. Ju, Numerical experiments on reaction front propagation in n-heptane/air mixture with temperature gradient, Proc. Combust. Inst. 35 (2015) 3045–3052.

[26] M. Faghih, X. Gou, Z. Chen, The explosion characteristics of methane, hydrogen and their mixtures: a computational study, J. Loss Prev. Process Ind. 40 (2016) 131–138.

[27] Z. Chen, Effects of radiation absorption on spherical flame propagation and radiation-induced uncertainty in laminar flame speed measurement, Proc. Combust. Inst. 36 (2017) 1129–1136.

[28] H. Yu, C. Qi, Z. Chen, Effects of flame propagation speed and chamber size on end-gas autoignition, Proc. Combust. Inst. 36 (2017) 3533–3541.

[29] Z. Chen, M.P. Burke, Y. Ju, Effects of compression and stretch on the determination of laminar flame speeds using propagating spherical flames, Combust. Theor. Model. 13 (2009) 343–364.

[30] P. Glarborg, A.B. Bendtsen, J.A. Miller, Nitromethane dissociation: implications for the $CH_3 + NO_2$ reaction, Int. J. Chem. Kinet. 31 (1999) 591–602.

[31] Z. Tian, L. Zhang, Y. Li, T. Yuan, F. Qi, An experimental and kinetic modeling study of a premixed nitromethane flame at low pressure, Proc. Combust. Inst. 32 (2009) 311–318.

[32] K. Zhang, Y. Li, T. Yuan, J. Cai, P. Glarborg, F. Qi, An experimental and kinetic modeling study of premixed nitromethane flames at low pressure, Proc. Combust. Inst. 33 (2011) 407–414.

[33] E.S. Starkman, Nitroparaffins as potential engine fuel, Ind. Eng. Chem. 51 (1959) 1477–1480.

[34] H. Yu, W. Han, J. Santner, X. Gou, C.H. Sohn, Y. Ju, Z. Chen, Radiation-induced uncertainty in laminar flame speed measured from propagating spherical flames, Combust. Flame 161 (2014) 2815–2824.

[35] S. Balusamy, A. Cessou, B. Lecordier, Direct measurement of local instantaneous laminar burning velocity by a new PIV algorithm, Exp. Fluids 50 (2011) 1109–1121.

[36] E. Varea, V. Modica, A. Vandel, B. Renou, Measurement of laminar burning velocity and Markstein length relative to fresh gases using a new postprocessing procedure: application to laminar spherical flames for methane, ethanol and isooctane/air mixtures, Combust. Flame 159 (2012) 577–590.

[37] E. Varea, J. Beeckmann, H. Pitsch, Z. Chen, B. Renou, Determination of burning velocities from spherically expanding H_2/air flames, Proc. Combust. Inst. 35 (2015) 711–719.

[38] E. Varea, V. Modica, B. Renou, A.M. Boukhalfa, Pressure effects on laminar burning velocities and Markstein lengths for isooctane–ethanol–air mixtures, Proc. Combust. Inst. 34 (2013) 735–744.

[39] D. Davidenko, R. Mével, G. Dupré, Numerical study of the detonation structure in rich H_2-NO_2/N_2O_4 and very lean H_2-N_2O mixtures, Shock Waves 21 (2011) 85–99.

[40] Y. Zhang, O. Mathieu, E.L. Petersen, G. Bourque, H.J. Curran, Assessing the predictions of a NO_x kinetic mechanism on recent hydrogen and syngas experimental data, Combust. Flame 182 (2017) 122–141.